DOI: 10.1002/ejoc.200700953

Nucleophilic Substitution at C, Si and P: How Solvation Affects the Shape of Reaction Profiles

Marc A. van Bochove[a] and F. Matthias Bickelhaupt*[a]

Keywords: Density functional calculations / Nucleophilic substitution / Phosphorus / Reaction mechanisms / Silicon / Solvent effects

We have studied how solvation affects the shape of potential energy surfaces (PES) of archetypal nucleophilic substitution reactions at carbon (S_N2@C), silicon (S_N2@Si) and phosphorus (S_N2@P), using the generalized gradient approximation (GGA) of density functional theory (DFT) at OLYP/TZ2P. Our model systems cover nucleophilic substitution, in water and in the gas phase, at carbon in $X^- + CH_3Y$ (S_N2@C), at silicon in $X^- + SiH_3Y$ (S_N2@Si), at tricoordinate phosphorus in $X^- + PR_2Y$ (S_N2@P3), and at tetracoordinate phosphorus in $X^- + POR_2Y$ (S_N2@P4) with substituents R = H, F, Cl, CH_3, OCH_3. In the gas phase, particular types of S_N2 reactions are characterized by different shapes of reaction profiles, such as single-, double- and triple-well PESs. The main effect of solvation is to turn the PESs of the S_N2@C but also of S_N2@Si and S_N2@P into unimodal reaction profiles which lead from the reactants via one single barrier to the products. The results are discussed in terms of differential solvation of reactants and transition states. We also address the question how the *relative* heights of reaction barriers are affected by solvation.
(© Wiley-VCH Verlag GmbH & Co. KGaA, 69451 Weinheim, Germany, 2008)

Introduction

Bimolecular nucleophilic substitution[1] at carbon (S_N2@C: see Scheme 1, A = C) has been studied extensively, both in the gas phase and in solution.[2,3] Most of chemistry occurs in solution. However, by revealing the intrinsic reactivity of model reactions, it is the gas-phase studies that have contributed much to our understanding of how solvation exactly affects the progress of reactions.

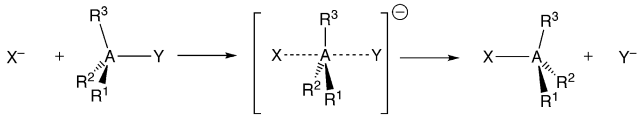

Scheme 1. Model S_N2 Reactions at A = C, Si, P.

In the absence of solvent, the reaction profile of a typical S_N2@C model reaction (e.g., $Cl^- + CH_3Cl$) is a double-well potential energy surface (PES), involving a reactant complex (RC) and a product complex (PC) separated by a central transition state (TS, see Figure 1, a).[2] Solvation causes this double-well PES to turn into a unimodal PES, with no (or only weakly pronounced) reactant and product complexes (see Figure 1, d).[2,3] The mechanism behind this solvent effect on the reaction profile is differential solvation of reactants and transition state: as the charge in the reactants is more localized, they are more strongly stabilized than the TS.[2a]

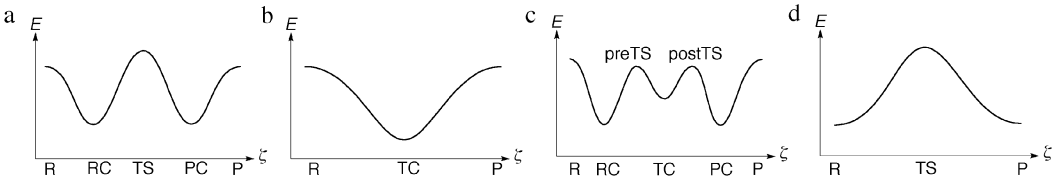

Figure 1. Types of reaction profiles, i.e., energy *E* vs. reaction coordinate ζ: (a) double-well, (b) single-well, (c) triple-well, (d) unimodal. R = reactants, RC = reactant complex, TS = transition state, TC = stable transition complex, PC = product complex, P = products.

[a] Theoretische Chemie, Scheikundig Laboratorium der Vrije Universiteit,
De Boelelaan 1083, 1081 HV Amsterdam, The Netherlands
Fax: +31-20-59-87629
E-mail: fm.bickelhaupt@few.vu.nl
Supporting information for this article is available on the WWW under http://www.eurjoc.org or from the author.

Much less studies have been devoted to understanding nucleophilic substitution at silicon (S_N2@Si)[4] and phosphorus (S_N2@P)[5] and how they are altered by solvation (see Scheme 1, A = Si and P, respectively). The reaction profile of small (e.g., R = H), archetypal S_N2@Si and

 © 2008 Wiley-VCH Verlag GmbH & Co. KGaA, Weinheim

Table 1. Energies (kcal mol^{-1}) relative to reactants of stationary points along the PES of various symmetric S_N2 reactions in the gas phase and in solution.[a]

No.	Reaction	Species[b]	Shape of PES	Gas phase[c]			Solution[d]
				RC	preTS	TS/TC	TS
1	$Cl^- + CH_3Cl$	**1**, **2**	double well	–9.0	–	–0.1	19.9
2	$Cl^- + SiH_3Cl$	**3**, **4**	single well	–	–	–24.4	3.0
3	$Cl^- + PH_2Cl$	**5**, **6**	single well	–	–	–26.2	0.2
4	$Cl^- + POH_2Cl$	**7**, **8**	single well	–	–	–22.3	8.2
5	$Cl^- + PF_2Cl$	**9**, **10**	single well	–	–	–24.7	5.5
6	$Cl^- + POF_2Cl$	**11**, **12**	single well	–	–	–13.6	20.2
7	$Cl^- + PCl_2Cl$	**13**, **14**	single well	–	–	–23.3	6.8
8	$Cl^- + POCl_2Cl$	**15**, **16**	triple well	–17.5	–2.0	–8.4	23.8
9	$Cl^- + P(CH_3)_2Cl$	**17**, **18**	triple well	–13.0	–12.7	–15.6	8.6
10	$Cl^- + PO(CH_3)_2Cl$	**19**, **20**	double well	–16.2	–	–5.7	20.7
11	$Cl^- + PO(OCH_3)_2Cl$	**21**, **22**	double well	–14.1	–	2.5	23.7

[a] Computed at OLYP/TZ2P. [b] See Figure 2 for structures. [c] Data from ref.[5a] [d] Water modeled with COSMO.[9] All solution-phase PESs are unimodal.

S_N2@P reactions in the gas phase is characterized by a single-well with a stable, hypervalent transition complex (TC, see Figure 1, b)[4,5] instead of a labile TS which features in the corresponding S_N2@C reactions. Interestingly, the introduction of sterically more demanding substituents (e.g., R = Cl) causes the appearance of pre- and post-transition states, separating the stable, hypervalent TC from reactant and product complexes.[4a,5a–5b] This constitutes a triple-well PES (Figure 1, c). Eventually, if the steric congestion becomes sufficiently large, pre- and post-barriers can merge into one central barrier which causes the pentavalent transition structure to turn from a stable TC into a labile TS (e.g., R = OCH_3). Thus, sterically crowded S_N2@Si and S_N2@P reactions begin to show S_N2@C-like behavior with double-well reaction profiles (Figure 1, a).[4a,5a]

Here, we address the question how solvation affects the reaction profiles of S_N2@Si and S_N2@P substitution. Is the effect of differential solvation similar to the situation known for S_N2@C? Is it able to smooth out all characteristic features (single-, double- and triple-well shape) of the S_N2@Si and S_N2@P gas-phase potential energy surfaces and to enforce one common, unimodal appearance of reaction profiles for nucleophilic substitution at each of the three investigates central atoms? And how are trends in relative reactivity of S_N2@C, S_N2@Si and S_N2@P substitution influenced by the solvent? To tackle these questions, we have computationally explored 11 model reactions in water and in the gas phase (see reactions 1–11 in Table 1). The model reactions cover nucleophilic substitution at carbon (S_N2@C), silicon (S_N2@Si), tricoordinate phosphorus (S_N2@P3) and tetracoordinate phosphorus (S_N2@P4). Our computations are based on the generalized gradient approximation (GGA) of density functional theory (DFT)[6] at OLYP/TZ2P.[7] This level of theory was previously shown to agree within a few kcal mol^{-1} with highly correlated ab initio benchmarks.[8] Solvation effects were treated using the conductor-like screening model (COSMO).[9]

Our investigations reveal a pronounced differential solvation effect in which reactants are more strongly solvated than transition states, also for S_N2@Si and S_N2@P reactions. Interestingly, the solvation energies of reactants are relatively constant whereas solvation energies in transition states show more pronounced variations. Thus, in many cases where solvation changes trends in relative reactivity, this counteracting solvent effect originates from the transition states.

Computational Methods

All calculations are based on density functional theory (DFT)[6] and have been carried out with the Amsterdam Density Functional (ADF) program.[10] Geometries and relative energies of the stationary points along the PESs of our model reactions as well as vibrational analyses thereof, to confirm equilibrium structures (no imaginary frequencies) or transition states (one imaginary frequency), were computed with the generalized gradient approximation (GGA) of DFT using the OLYP functional which involves the optimized exchange (OPTX) functional proposed by Handy and co-workers,[7a–7b] and the Lee–Yang–Parr (LYP) correlation functional.[7c] Recently, we have shown that OLYP agrees within a few kcal mol^{-1} with highly correlated ab initio benchmarks.[8] The molecular orbitals (MOs) were expanded in a large uncontracted set of Slater-type orbitals (STOs) containing diffuse functions, TZ2P. The TZ2P basis set is of triple-ζ quality and has been augmented with two sets of polarization functions: 2*p* and 3*d* on hydrogen, 3*d* and 4*f* on carbon, oxygen, fluorine, silicon, phosphorus and chlorine. The core shells of carbon, oxygen, fluorine (1*s*), silicon, phosphorus and chlorine (1*s*2*s*2*p*) were treated by the frozen-core approximation, that is, they are excluded from the variational optimization.[10b] An auxiliary set of *s*, *p*, *d*, *f* and *g* STOs was used to fit the molecular density and to represent the Coulomb and exchange potentials accurately in each SCF cycle.[10b,10d]

Solvent effects were taken into account in all condensed-phase calculations using the COSMO model,[9] used explicitly in the solving of the SCF equations, the optimization of the geometry and the vibrational analysis. The solvent radius (R_s) for water was taken from experimental data for the macroscopic density (ρ) and molecular mass (M_m)

 © 2008 Wiley-VCH Verlag GmbH & Co. KGaA, Weinheim

with the formula $R_s^3 = 2.6752 \cdot M_m/\rho$, leading to a R_s value of 1.9 Å for water; a value of 78.4 was used for the dielectric constant of water. Atomic radii values were taken from the MM3 van der Waals radii,[11] which are available for almost the whole periodic system, and scaled by 0.8333 (the MM3 radii are 20% larger than the normal van der Waals radii due to the specific form for the van der Waals energy within the MM3 force field). The surface charges at the GEPOL93 solvent-excluding surface[12] were corrected for outlying charges. This setup provides a "non-empirical" approach to including solvent effects with a dielectric continuum, and works well for solvation processes.[13] The file needed for including this setup in a COSMO computation with the ADF program (including all values of the above-mentioned atomic radii) is provided in Table S1 of the electronic supporting information.

Results and Discussion

The results of our aqueous solution-phase OLYP/TZ2P computations are collected, together with the corresponding gas-phase data from earlier work,[5a] in Table 1 and Table 2 (energies and analyses) and Figure 2 (structures). Cartesian coordinates for all stationary points in solution are provided in Table S2 of the electronic supporting information.

Our results for the S_N2@C reaction of Cl^- + CH_3Cl nicely confirm the well-known[2,3] switch from a double-well potential in the gas phase to a unimodal reaction profile in solution: the overall barrier increases from –0.1 kcal mol^{-1} in the gas phase to 19.9 kcal mol^{-1} in water (see reaction 1 in Table 1). Importantly, solvation also turns the *single-well* potential energy surfaces of the corresponding S_N2@Si reaction of Cl^- + SiH_3Cl and that of the S_N2@P3 reaction of Cl^- + PH_2Cl in the gas phase to unimodal ones in water (see reactions 2 and 3 in Table 1). Note however that the solution-phase reaction profiles of reactions 2 and 3 are extremely shallow. In the case of reaction 2, the D_{3h} symmetric transition state **4** is only 3 kcal mol^{-1} above the reactants Cl^- + SiH_3Cl. In this particular case, but in none of the other solution-phase transition states, this leads to a numerical artefact, namely, a shift of the small imaginary frequency associated with the transition vector of **4** to a slightly positive value (38 cm^{-1}). In the case of reaction 3, the C_{2v} symmetric transition state **6** is only 0.2 kcal mol^{-1} above the reactants Cl^- + PH_2Cl. Thus, in aqueous solution, S_N2@Si and S_N2@P substitution adopt, just as S_N2@C, unimodal reaction profiles, be it with far less pronounced maxima than the latter. Still this implies a significant differential solvation in which the stabilization of the S_N2@Si and S_N2@P reactants is roughly 27 kcal mol^{-1} greater than that of the TS.

It was shown previously that the hypervalent transition structure of S_N2@Si or S_N2@P reactions is destabilized if the steric congestion around the central Si or P atom increases.[4a,5a] This trend is in many but not all cases preserved. For example, along the series of S_N2@P3 reactions of Cl^- + PH_2Cl, PCl_2Cl and $P(CH_3)_2Cl$ the energy of the transition species relative to reactants increases, both in the gas phase (from –26.2 to –23.3 to –15.6 kcal mol^{-1}) and in aqueous solution from 0.2 to 6.8 to 8.6 kcal mol^{-1}; see reactions 3, 7, 9 in Table 1. Note however that while these reactions proceed via a single-well PES in the gas phase, they have again a unimodal reaction profile in solution.

Likewise, increasing the coordination number of phosphorus in the substrate from 3 to 4 raises the energy of the transition species. Thus, going from the S_N2@P3 reaction of Cl^- + PH_2Cl to the S_N2@P4 reaction of Cl^- + POH_2Cl, the energy of the transition species increases from –26.2 to –22.3 kcal mol^{-1} in the gas phase and from 0.2 to 8.2 kcal mol^{-1} in solution (see reactions 3, 4 in Table 1).

A discrepancy between gas- and condensed-phase trends arises if we further increase the steric demand of the substituents around phosphorus along the S_N2@P4 reactions of Cl^- + POH_2Cl, $POCl_2Cl$, $PO(CH_3)_2Cl$ and $PO(OCH_3)_2Cl$ (reactions 4, 8, 10, 11 in Table 1). In the gas phase, the en-

Table 2. Net solvation energies ΔE_{solv} (kcal mol^{-1}), chlorine atomic charge Q_{Cl} (a.u.) and A–Cl distance (Å) of individual reactants and transition states in solution.[a]

		Reactants[b]			Transition state		
No.	Reaction	ΔE_{solv}	Q_{Cl}	A–Cl	ΔE_{solv}	Q_{Cl}	A–Cl
–	Cl^-	–75.29[c]	–1.000[c]	–	–	–	–
1	Cl^- + CH_3Cl	–0.81	–0.170	1.80	–56.04	–0.578	2.35
2	Cl^- + SiH_3Cl	–1.28	–0.208	2.09	–49.09	–0.510	2.38
3	Cl^- + PH_2Cl	–0.99	–0.185	2.10	–49.92	–0.524	2.42
4	Cl^- + POH_2Cl	–9.28	–0.093	2.03	–54.00	–0.474	2.36
5	Cl^- + PF_2Cl	–2.39	–0.146	2.08	–47.48	–0.517	2.42
6	Cl^- + POF_2Cl	–6.35	0.020	1.97	–47.84	–0.380	2.25
7	Cl^- + PCl_2Cl	–0.90	–0.113	2.08	–46.17	–0.514	2.46
8	Cl^- + $POCl_2Cl$	–4.56	–0.008	2.01	–47.64	–0.398	2.32
9	Cl^- + $P(CH_3)_2Cl$	–1.25	–0.210	2.12	–52.33	–0.542	2.51
10	Cl^- + $PO(CH_3)_2Cl$	–8.66	–0.138	2.07	–57.59	–0.511	2.51
11	Cl^- + $PO(OCH_3)_2Cl$	–7.06	–0.109	2.05	–61.09	–0.567	2.53

[a] Computed at OLYP/TZ2P. Net solvation energy of species X corresponds to reaction X(g)→X(aq). Q_{Cl} values obtained for X(aq) with VDD method[14] (Q_{Cl} values of the same solution-phase structures but in absence of solvent are only slightly, i.e., 0.00–0.05 a.u. less polarized and show the same trend; see Table S3 in the electronic supporting information). [b] Values refer to substrate unless stated otherwise. [c] Values refer to the chloride anion.

 © 2008 Wiley-VCH Verlag GmbH & Co. KGaA, Weinheim

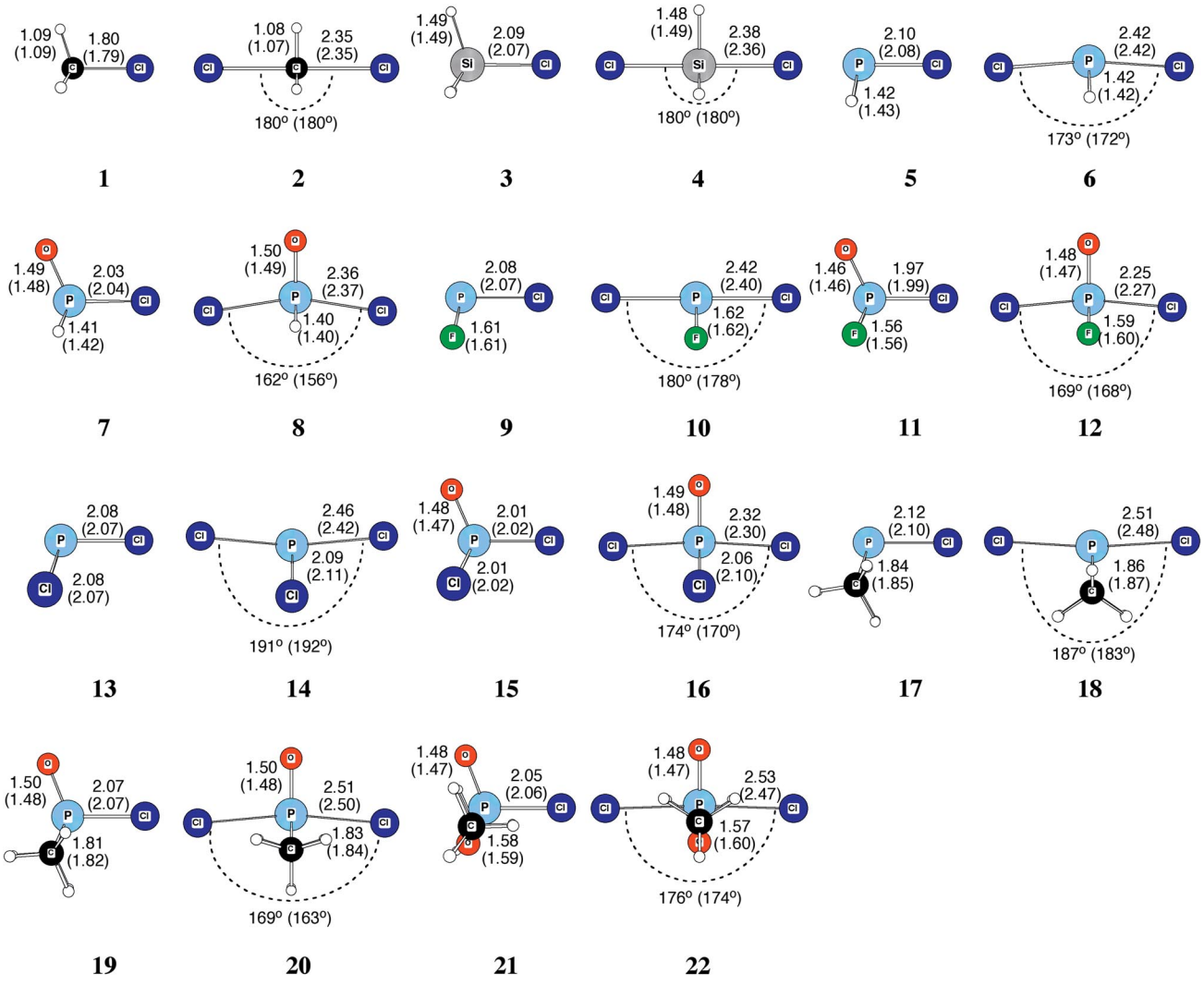

Figure 2. Structures (units Å, deg) of stationary points along S_N2 reactions 1–11 in solution (see Table 1). Values in parentheses refer to corresponding gas-phase geometry.

ergy of the transition species increases monotonically along this series, from –22.3 to –8.4 to –5.7 to 2.5 kcal mol^{-1} and the shape of the PES changes from single-well via triple-well to double-well (compare parts b, c, a in Figure 1). In solution, however, the trend of destabilization occurs only from Cl^- + POH_2Cl (8.2 kcal mol^{-1}) to Cl^- + $POCl_2Cl$ (23.8 kcal mol^{-1}). Thereafter, along Cl^- + $POCl_2Cl$, $PO(CH_3)_2Cl$ and $PO(OCH_3)_2Cl$, the transition species is slightly *stabilized* (instead of being further *destabilized*), from 23.8 to 20.7 to 23.7 kcal mol^{-1} (see reactions 8, 10, 11 in Table 1).

Interestingly, the solvent-induced change in the trend of relative energies of transition species appears to originate from variations in the solvation energies ΔE_{solv} of the transition species, and not from variations in the much larger solvation energies of the reactants (see Table 2). We discuss the set of S_N2@P4 reactions Cl^- + $POCl_2Cl$ and Cl^- + $PO(CH_3)_2Cl$, along which the effect is quite pronounced (see reactions 8 and 10 in Table 1 and Table 2). Thus, in the gas phase the transition species is destabilized along this series by about 3 kcal mol^{-1} whereas in solution it is *stabilized* by about 3 kcal mol^{-1} (see reactions 8 and 10 in Table 1).

Inspection of Table 2 shows that here (and also in the other reactions), the solvation energy of the reactants is dominated by the large and constant contribution of –75 kcal mol^{-1} from chloride whereas the solvation energies of the neutral substrates are small, i.e., –9 kcal mol^{-1} or less, and variations are therefore also small (ca 8 kcal mol^{-1}). This holds in particular within a structurally related series such as the example we are discussing here: from reaction 8 to 10, the solvation energy of the substrates $POCl_2Cl$ and $PO(CH_3)_2Cl$, respectively, becomes only slightly more stabilizing, i.e., ΔE_{solv} goes from –4.6 to –8.7 kcal mol^{-1} (see Table 2). Note, by the way, that as such this effect would destabilize the relative energy of the transition species in solution while it turns out to be stabilized.

Thus, the inversion on the trend must come from the solvation of the transition species. Indeed, as can be seen in Table 2, the solvation energies of the transition species

 © 2008 Wiley-VCH Verlag GmbH & Co. KGaA, Weinheim

ΔE_{solv}(TS) are smaller than those of the reactants ΔE_{solv}(R) (differential solvation, vide supra) but the variation in ΔE_{solv}(TS) along all model reactions is twice as large as ΔE_{solv}(R): ca. 15 vs. 8 kcal mol^{-1}. Along the S_N2@P4 reactions 8 and 10, we see that ΔE_{solv}(TS) becomes 10 kcal mol^{-1} more stabilizing. This variation in ΔE_{solv}(TS) overrules the opposite but smaller variation in ΔE_{solv}(R) and is responsible for the fact that in aqueous solution, the barrier for the S_N2@P4 reaction of Cl^- + $PO(CH_3)_2Cl$ is lower than that for Cl^- + $POCl_2Cl$ (see reactions 8 and 10 in Table 1 and Table 2).

Similar inversions in trend from gas to condensed phase, all caused by counteracting trends in ΔE_{solv}(TS), can also be observed for other sets of reactions. This leads to the interesting notion, already mentioned above and graphically illustrated by Figure 3, that, although smaller than the solvation energies of the reactants (cf. differential solvation), the solvation energies of transition states are responsible in our model reactions for solvent-induced changes in reactivity trends as compared to the gas phase.

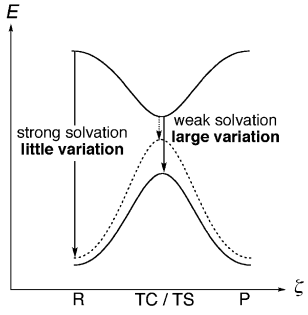

Figure 3. Differential solvation exemplified for gas-phase single-well PES: reactants are solvated more strongly than transition states leading to a unimodal PES in solution. But the solvation energy of transition states shows larger variation from one model reaction to another.

Finally, we address the question *why* the solvation energy of the transition species becomes more stabilizing from reaction 8 to 10, i.e., from species **16** to **20**, in spite of the fact that we replace the more polar chlorine substituents in $POCl_2Cl$ by the larger and less polar methyl substituents in $PO(CH_3)_2Cl$. As pointed out previously, the increased steric bulk associated with this substitution causes the destabilization of **20** relative to **16** in the gas phase. But the increased steric congestion in **20** also causes the axial P–Cl bonds to expand by a sizeable 0.2 Å, that is, from 2.32 Å in **16** to 2.51 Å in **20** (see Table 2 and Figure 2). The longer P–Cl bonds cause an increase in the chlorine atomic charge (–0.398 a.u. in **16** vs. –0.511 a.u. in **20**) and, in addition, it causes the anionic chlorine atoms to be somewhat more exposed to the solvent. This in turn enhances the interaction with the solvent which translates into a net stabilization of ΔE_{solv}(TS) from **16** to **20** (see Table 2). Similar mechanisms can be observed in other sets of reactions that show a solvent-induced change of the trend in relative stabilities of the transition species.

Conclusions

Solvation drastically raises barriers and straightens out all structure from the reaction profiles of the investigated model S_N2@C, S_N2@Si and S_N2@P reactions. In the gas phase, particular types of S_N2 reactions are characterized by different shapes of reaction profiles, such as single-, double- and triple-well PESs which may feature negative activation energies. Solvation turns the PESs of S_N2@C but also of S_N2@Si and S_N2@P reactions into unimodal reaction profiles which lead from the reactants via one single barrier, with a positive overall activation energy, to the products.

Trends that occur along homologous series in the gas phase are, in some cases, preserved in solution. One example is the raise in energy of the transition species that is generally observed if one goes from the nucleophilic substitutions of Cl^- + PR_2Cl (i.e., at a tricoordinate phosphorus: S_N2@P3) to the corresponding substitution reactions of Cl^- + POR_2Cl (i.e., at a tetracoordinate phosphorus: S_N2@P4).

But solvation can also change relative heights in reaction barriers. Such a change in relative barrier heights is in many cases caused by trends in the solvation energy of the transition state, ΔE_{solv}(TS), that counteract the trend in gas-phase barriers. This is interesting because ΔE_{solv}(TS) is in general weaker than the solvation energy of the reactants, ΔE_{solv}(R). The point is, however, that the *variations* in ΔE_{solv}(TS) are larger than those in ΔE_{solv}(R).

Supporting Information (see also the footnote on the first page of this article): COSMO settings (including atomic radii), Cartesian coordinates and energies of all solvated species, and chlorine atomic charge of selected structures are available as Supporting Information.

Acknowledgments

We thank the National Research School Combination – Catalysis (NRSC-C) and the Netherlands Organization for Scientific Research (NWO-CW and NWO-NCF) for financial support.

[1] a) M. B. Smith, J. March, *March's Advanced Organic Chemistry*, 6th ed., Wiley-Interscience, New York, **2007**; b) F. A. Carey, R. J. Sundberg, *Advanced Organic Chemistry*, 4th ed., Springer, New York, **2006**.

[2] a) J. K. Laerdahl, E. Uggerud, *Int. J. Mass Spectrom.* **2002**, *214*, 277–314; b) S. Schmatz, *ChemPhysChem* **2004**, *5*, 600–617; c) W. N. Olmstead, J. I. Brauman, *J. Am. Chem. Soc.* **1977**, *99*, 4219–4228; d) M. L. Chabinyc, S. L. Craig, C. K. Regan, J. I. Brauman, *Science* **1998**, *279*, 1882–1886; e) F. M. Bickelhaupt, *J. Comput. Chem.* **1999**, *20*, 114–128; f) E. Uggerud, *Chem. Eur. J.* **2006**, *12*, 1127–1136; g) J. M. Gonzales, W. D. Allen, H. F. Schaefer III, *J. Phys. Chem. A* **2005**, *109*, 10613–10628; h) J. M. Gonzales, C. Pak, R. S. Cox, W. D. Allen, H. F. Schaefer III, A. G. Csaszar, G. Tarczay, *Chem. Eur. J.* **2003**, *9*, 2173–2192; i) S. Gronert, *Acc. Chem. Res.* **2003**, *36*, 848–857; j) S. Gronert, *Chem. Rev.* **2001**, *101*, 329–360; k) P. Botschwina, *Theor. Chem. Acc.* **1998**, *99*, 426–428; l) W. L. Hase, *Science* **1994**, *266*, 998–1002; m) L. Q. Deng, V. Branchadell, T. Ziegler, *J. Am. Chem. Soc.* **1994**, *116*, 10645–10656; n) N. M. M. Nibbering, *Acc. Chem. Res.* **1990**, *23*, 279; o) N. M. M. Nibbering, *Adv. Phys. Org. Chem.* **1988**, *24*, 1; p) J. M. Riveros, S. M. Jose, K. Takashima, *Adv. Phys. Org. Chem.* **1985**, *21*, 197.

 © 2008 Wiley-VCH Verlag GmbH & Co. KGaA, Weinheim

[3] a) L. Song, W. Wu, P. C. Hiberty, S. Shaik, *Chem. Eur. J.* **2006**, *12*, 7458–7466; b) B. Bogdanov, T. B. McMahon, *Int. J. Mass Spectrom.* **2005**, *241*, 205–223; c) G. Vayner, K. N. Houk, W. L. Jorgensen, J. I. Brauman, *J. Am. Chem. Soc.* **2004**, *126*, 9054–9058; d) B. Ensing, E. J. Meijer, P. E. Blöchl, E. J. Baerends, *J. Phys. Chem. A* **2001**, *105*, 3300–3310; e) Y. Mo, J. Gao, *J. Comput. Chem.* **2000**, *21*, 1458–1469; f) T. N. Truong, E. V. Stefanovich, *J. Phys. Chem.* **1995**, *99*, 14700–14706; g) J. Chandrasekhar, S. F. Smith, W. L. Jorgensen, *J. Am. Chem. Soc.* **1985**, *107*, 154–163.

[4] a) A. P. Bento, F. M. Bickelhaupt, *J. Org. Chem.* **2007**, *72*, 2201–2207; b) R. R. Holmes, *Chem. Rev.* **1996**, *96*, 927–950; c) R. Damrauer, J. A. Hankin, *Chem. Rev.* **1995**, *95*, 1137–1160; d) T. L. Windus, M. S. Gordon, L. P. Davis, L. W. Burggraf, *J. Am. Chem. Soc.* **1994**, *116*, 3568–3579; e) J. C. Sheldon, R. N. Hayes, J. H. Bowie, *J. Am. Chem. Soc.* **1984**, *106*, 7711–7715.

[5] a) M. A. van Bochove, M. Swart, F. M. Bickelhaupt, *J. Am. Chem. Soc.* **2006**, *128*, 10738–10744; b) M. A. van Bochove, M. Swart, F. M. Bickelhaupt, *ChemPhysChem* **2007**, *8*, 2452–2463; c) T. I. Sølling, A. Pross, L. Radom, *Int. J. Mass Spectrom.* **2001**, *210*, 1–11; d) S. M. Bachrach, D. C. Mulhearn, *J. Phys. Chem.* **1993**, *97*, 12229–12231; e) C. Fish, M. Green, R. J. Kilby, J. M. Lynam, J. E. McGrady, D. A. Pantazis, C. A. Russell, A. C. Whitwood, C. E. Willans, *Angew. Chem.* **2006**, *118*, 3710–3713; *Angew. Chem. Int. Ed.* **2006**, *45*, 3628–3631; f) K. C. Kumara Swamy, N. Satish Kumar, *Acc. Chem. Res.* **2006**, *39*, 324–333; g) R. R. Holmes, *Acc. Chem. Res.* **2004**, *37*, 746–753; h) S. Humbel, C. Bertrand, C. Darcel, C. Bauduin, S. Juge, *Inorg. Chem.* **2003**, *42*, 420–427; i) J. Florian, A. Warshel, *J. Phys. Chem. B* **1998**, *102*, 719–734; j) J. L. Li, P. Beak, *J. Am. Chem. Soc.* **1992**, *114*, 9206–9207; k) C. Lim, M. Karplus, *J. Am. Chem. Soc.* **1990**, *112*, 5872–5873; l) E. P. Kyba, *J. Am. Chem. Soc.* **1975**, *97*, 2554–2555; m) N. Iché-Tarrat, M. Ruiz-Lopez, J.-C. Barthelat, A. Vigroux, *Chem. Eur. J.* **2007**, *13*, 3617–3629; n) K. Range, M. J. McGrath, X. Lopez, D. M. York, *J. Am. Chem. Soc.* **2004**, *126*, 1654–1665.

[6] a) R. G. Parr, W. Yang, *Density Functional Theory of Atoms and Molecules*, Oxford University Press, New York, **1989**; b) W. Koch, M. C. Holthausen, *A Chemist's Guide to Density Functional Theory*, Wiley-VCH, Weinheim, **2000**; c) R. Dreizler, E. Gross, *Density Functional Theory*, Plenum Press, New York, **1995**; d) F. M. Bickelhaupt, E. J. Baerends, *Rev. Comput. Chem.* **2000**, *15*, 1–86; e) E. J. Baerends, O. V. Gritsenko, *J. Phys. Chem. A* **1997**, *101*, 5383–5403; f) T. Ziegler, *Can. J. Chem.* **1995**, *73*, 743–761; g) T. Ziegler, *Chem. Rev.* **1991**, *91*, 651–667.

[7] a) N. C. Handy, A. J. Cohen, *J. Chem. Phys.* **2002**, *116*, 5411–5418; b) N. C. Handy, A. J. Cohen, *Mol. Phys.* **2001**, *99*, 403–412; c) C. T. Lee, W. T. Yang, R. G. Parr, *Phys. Rev. B* **1988**, *37*, 785–789.

[8] a) A. P. Bento, M. Solà, F. M. Bickelhaupt, *J. Comput. Chem.* **2005**, *26*, 1497–1504; b) M. Swart, M. Solà, F. M. Bickelhaupt, *J. Comput. Chem.* **2007**, *28*, 1551–1560.

[9] a) A. Klamt, G. Schüürmann, *J. Chem. Soc. Perkin Trans. 2* **1993**, 799–805; b) A. Klamt, *J. Phys. Chem.* **1995**, *99*, 2224–2235; c) C. C. Pye, T. Ziegler, *Theor. Chem. Acc.* **1999**, *101*, 396–408.

[10] a) G. te Velde, F. M. Bickelhaupt, E. J. Baerends, C. Fonseca Guerra, S. J. A. van Gisbergen, J. G. Snijders, T. Ziegler, *J. Comput. Chem.* **2001**, *22*, 931–967; b) *Computer code ADF 2006.01*: E. J. Baerends, J. Autschbach, A. Bérces, J. A. Berger, F. M. Bickelhaupt, C. Bo, P. L. de Boeij, P. M. Boerrigter, L. Cavallo, D. P. Chong, L. Deng, R. M. Dickson, D. E. Ellis, M. van Faassen, L. Fan, T. H. Fischer, C. Fonseca Guerra, S. J. A. van Gisbergen, J. A. Groeneveld, O. V. Gritsenko, M. Grüning, F. E. Harris, P. van den Hoek, C. R. Jacob, H. Jacobsen, L. Jensen, E. S. Kadantsev, G. van Kessel, R. Klooster, F. Kootstra, E. van Lenthe, D. A. McCormack, A. Michalak, J. Neugebauer, V. P. Nicu, V. P. Osinga, S. Patchkovskii, P. H. T. Philipsen, D. Post, C. C. Pye, W. Ravenek, P. Romaniello, P. Ros, P. R. T. Schipper, G. Schreckenbach, J. G. Snijders, M. Solà, M. Swart, D. Swerhone, G. te Velde, P. Vernooijs, L. Versluis, L. Visscher, O. Visser, F. Wang, T. A. Wesolowski, E. M. van Wezenbeek, G. Wiesenekker, S. K. Wolff, T. K. Woo, A. L. Yakovlev, T. Ziegler, SCM, Amsterdam, The Netherlands; c) E. J. Baerends, D. E. Ellis, P. Ros, *Chem. Phys.* **1973**, *2*, 41–51; d) C. Fonseca Guerra, J. G. Snijders, G. te Velde, E. J. Baerends, *Theor. Chem. Acc.* **1998**, *99*, 391–403.

[11] N. L. Allinger, X. Zhou, J. Bergsma, *J. Mol. Struct. (THEOCHEM)* **1994**, *312*, 69–83.

[12] a) J. L. Pascual-Ahuir, E. Silla, *J. Comput. Chem.* **1990**, *11*, 1047–1060; b) E. Silla, I. Tunon, J. L. Pascual-Ahuir, *J. Comput. Chem.* **1991**, *12*, 1077–1088; c) J. L. Pascual-Ahuir, E. Silla, I. Tunon, *J. Comput. Chem.* **1994**, *15*, 1127–1138.

[13] a) M. Swart, E. Rösler, F. M. Bickelhaupt, *Eur. J. Inorg. Chem.* **2007**, 3646–3654; b) R. S. Bon, B. van Vliet, N. E. Sprenkels, R. F. Schmitz, F. J. J. de Kanter, C. V. Stevens, M. Swart, F. M. Bickelhaupt, M. B. Groen, R. V. A. Orru, *J. Org. Chem.* **2005**, *70*, 3542–3553.

[14] a) F. M. Bickelhaupt, N. J. R. van Eikema Hommes, C. Fonseca Guerra, E. J. Baerends, *Organometallics* **1996**, *15*, 2923–2931; b) C. Fonseca Guerra, F. M. Bickelhaupt, J. G. Snijders, E. J. Baerends, *Chem. Eur. J.* **1999**, *5*, 3581–3594.

Received: October 8, 2007
Published Online: December 19, 2007

 © 2008 Wiley-VCH Verlag GmbH & Co. KGaA, Weinheim